Available online at www.sciencedirect.com
ScienceDirect
Nuclear Instruments and Methods in Physics Research B 266 (2008) 4167–4170
NIM B
Beam Interactions with Materials & Atoms
www.elsevier.com/locate/nimb

Improvements of the DRAGON recoil separator at ISAC

C. Vockenhuber [a,*], L. Buchmann [a], J. Caggiano [a,1], A.A. Chen [b], J.M. D'Auria [c], C.A. Davis [a], U. Greife [d], A. Hussein [e], D.A. Hutcheon [a], D. Ottewell [a], C.O. Ouellet [b], A. Parikh [f], J. Pearson [b], C. Ruiz [a], G. Ruprecht [a], M. Trinczek [a], J. Zylberberg [a]

[a] *TRIUMF, 4004 Wesbrook Mall, Vancouver, BC, Canada V6T 2A3*
[b] *McMaster University, Hamilton, ON, Canada*
[c] *Simon Fraser University, Burnaby, BC, Canada*
[d] *Colorado School of Mines, Golden, CO, USA*
[e] *University of Northern British Columbia, Prince George, BC, Canada*
[f] *Yale University, New Haven, CT, USA*

Available online 18 June 2008

Abstract

The DRAGON (Detector of Recoils And Gammas Of Nuclear reactions) is used to measure radiative proton and alpha capture reaction rates involving both stable and radioactive, heavy-ion reactants at the TRIUMF-ISAC high intensity radioactive beam facility. Completed in 2001 it has been used for several challenging studies for nuclear astrophysics, e.g. $^{12}C(\alpha, \gamma)^{16}O$, $^{21}Na(p, \gamma)^{22}Mg$, $^{26g}Al(p, \gamma)^{27}Si$ and $^{40}Ca(\alpha, \gamma)^{44}Ti$. Since initial operation, a number of improvements have been incorporated which are described here. These include a beam centering monitor based on a CCD camera, a mechanical iris to skim of beam halo, a solid state stripper acting as a charge state booster for beams with $A \gtrsim 30$, beta and gamma detectors to monitor beam intensity and to determine beam contamination in experiments with radioactive beam and the ionization chamber for both recoil identification and isobar separation.

PACS: 29.40.−n; 29.40.Cs; 29.30.−h

Keywords: Mass separator; Beta and gamma detector; Ionization chamber

1. Introduction

The DRAGON facility at TRIUMF-ISAC has been designed to measure radiative proton and alpha capture reaction of astrophysical interest. These reactions play an important role in many stellar nucleosynthesis scenarios including helium burning and explosive environments like novae, X-ray bursts and supernovae. The astrophysically relevant energies are typically several 100's of keV in center-of-mass; the ISAC-I accelerators provide beams with laboratory energies of 0.15–1.75 A MeV for measurements in inverse kinematics. Due to the low yield of reaction products of interest (here called recoils) relative to incoming beam particles, typically less than 10^{-10}, high beam intensities are needed to perform a measurement within a reasonable time frame. On the other hand, a high beam suppression after the reaction target is essential in order to see the few recoils.

The DRAGON facility consists of a windowless gas target followed by a two stage recoil spectrometer consisting of two magnetic and two electrostatic dipoles (Fig. 1). Recoils are detected at the final heavy ion detector and in coincidence with a gamma detection at the BGO detector array surrounding the gas target. A detailed description of the experimental setup and the commissioning of DRAGON can be found elsewhere [1,2]. The suppression of beam is the subject to another contribution to these

* Corresponding author.
E-mail address: christof.vockenhuber@triumf.ca (C. Vockenhuber).
[1] Present address: Pacific Northwest Nuclear Laboratory, Richland, WA, USA.

0168-583X/$ - see front matter © 2008 Elsevier B.V. All rights reserved.
doi:10.1016/j.nimb.2008.05.146

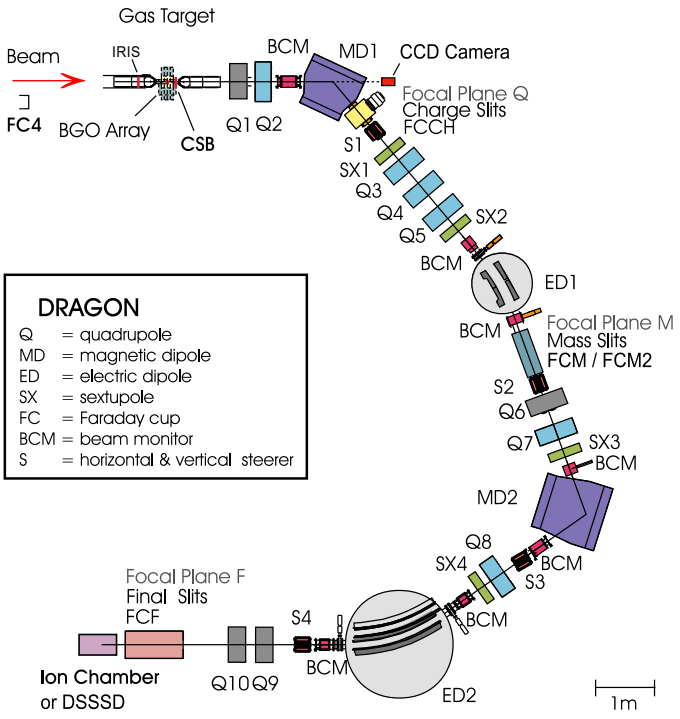

Fig. 1. Schematic layout of the DRAGON facility.

proceedings [3]. In this paper we describe the improvements to DRAGON which were developed to improve the performance of the facility. We start our description at the windowless gas target, where we installed a beam centering monitor, a mechanical iris to skim of any beam halo and a retractable solid stripper for boosting charge states for reactions with heavier beams. At the mass slits after the first electric dipole, where most of the beam is dumped, we installed several radiation detectors for monitoring intensity and contamination of radioactive beams. At the tail end of DRAGON we commissioned the ionization chamber and successfully used it for studying the ^{40}Ca(α, γ)^{44}Ti reaction.

2. Beam centering monitor

The beam coming from the ISAC-I accelerators are directed to the windowless gas target and should hit the gas target at the center. A well centered and small (about 2 mm) beam spot and a straight direction are important for the performance of the BGO detector array (see Section 3) and subsequent spectrometer (see [3] for details). We installed a telescope equipped with a sensitive CCD camera, MX7-C from Starlight Xpress, Holyport, England, at the straight port of the first magnetic dipole MD1 (Fig. 1). As the beam passes through the target cell it ionizes the gas and the beam spot becomes visible (Fig 2).

The direction of the beam is checked by comparing the beam position centroid with and without focusing of the first two quadrupoles (Q1 and Q2) at a wire scanner close to the focus position after MD1. The direction of the beam

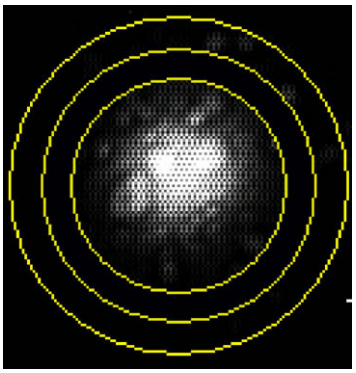

Fig. 2. CCD image of the beam spot at the gas target (^{40}Ca at 890 A keV, 2 pnA, 4.1 Torr He gas). The outer ring corresponds to the smallest aperture of 6 mm.

is adjusted by a pair of steerers in each direction upstream of the gas target until the centroid does not move during the quads on/off exercise. During this process the beam position is checked by the CCD camera.

The CCD image can be analyzed with regard of centroid and intensity of the beam spot by the software MaxIm DL from Diffraction Limited, Ontario, Canada. This allows to monitor both beam position and intensity during a measurement. The intensity output is clearly correlated with the beam intensity measured with the elastic monitors. However, in all the measurements we relied on our primary intensity monitors, i.e. collimated silicon detectors measuring elastically scattered gas atoms, current on the mass slit or the off-set Faraday cup FCM2 after ED1 in case of the ^{12}C(α, γ)^{16}O reaction [4].

3. Mechanical iris

One challenge in experiments with short-lived nuclides is beam deposited at the gas target which can cause high rates at the highly efficient BGO detector array. A well centered beam and a small beam spot at the gas target avoids that a substantial part of the beam is stopped inside or near the gas target. But even then, beam halo can lead to a beam spill. During the ^{26g}Al(p, γ)^{27}Si experiment [5] we had a significant activity from ^{26}Na ($t_{1/2} = 1.07$ s) contamination which was stopped and decayed near the gas target and thus increased random coincidences with the recoil detection. We therefore installed a mechanical iris from Edmund Optics, Barrington, NJ, USA, upstream of the gas target to skim off any beam halo. The opening of the iris can be adjusted from 2.3 to 19 mm and its position in x and y within $\pm$5 mm without breaking the vacuum. The iris was adjusted (typically with an opening of 4–5 mm) to reduce the background count rate at the BGO detector array by a factor of about 5 while keeping the beam transmission at $\sim$90% or above.

4. Charge state booster

The bending requirement of the electrostatic and magnetic dipoles limits the useable charge states at the recoil

separator. For the lighter masses ($A \lesssim 30$) the mean charge state after the gas target is usually well above the minimal usable charge state. However, for heavier masses the mean charge state is close or below this limit. For instance for the ^{40}Ca(α, γ)^{44}Ti reaction charge states around 11^+ (for ^{40}Ca at 1.12 A MeV) are populated whereas only the charge states above 13^+ can be bent by the dipoles.

To overcome this limitation we implemented a retractable foil stripper right after the inner gas cell (we called it charge state booster (CSB)). The basic idea is that solid stripping media result in higher charge states of passing ions. We use silicon nitride windows of 50 nm and 100 nm thickness (=17 and 34 μg/cm^2 respectively) from Silson Ltd., Northampton, UK, which are more robust against gas flow from the target cell compared to carbon foils of similar thickness. The life-time of a 100 nm SiN foil under ~1.1 MeV/u ^{40}Ca beam irradiation is up to 600 pnA h, significantly longer than the carbon foils used for stripping between the ISAC-1 accelerators.

Details and performance of the CSB are described in another paper [6].

5. Beta and gamma detectors for beam monitoring

In cross section measurements of this kind the determination of the incoming beam fluence is an important quantity. For a reliable quantification the beam intensity and its variation over time has to be known. For experiments with stable beam the intensity is usually high enough (well above 10^9 particle per seconds) to be reliably measured as a current in a Faraday cup. Radioactive beam is sometimes less intense by several orders of magnitude and thus resulting in a current in the pA range or even below. In addition, beam contamination by isobars can be significant contribution to the incoming beam intensity. This contamination depends on many parameters in the production target, ion source and high resolution mass separator and thus may vary substantially over the measuring time. Therefore, we installed several radiation detectors at the mass slits (x slits after ED1 where most of the incoming beam is dumped) which monitor beam intensity and beam purity during the measurement (Fig. 3).

Two 6 mm thick plastic scintillators have been installed upstream of the mass slits to detect beta particles from stopped and decaying beam particles in the ^{21}Na(p, γ)^{22}Mg experiment [7]. ^{21}Na beta decays with a half-life of 22.5 s. The monitors can be operated in coincidence mode and are calibrated by a current measurement of the high-intensity incoming ^{21}Na (up to ~10^9 s^{-1}). Because of the use of the surface ion source beam contamination was not an issue in the measurements with the ^{21}Na beam.

In case of the ^{26g}Al(p, γ)^{27}Si measurement [5], due to the long half-life of ^{26g}Al ($t_{1/2} = 7.2 \times 10^5$ yr) there are no useful activities for beam monitoring. However, beam contamination from ^{26}Na (1.07 s) and $^{26\,m}$Al (6.345 s) posed some challenges. We used a HPGe detector pointed at the mass slits to monitor the ^{26}Na component of the beam via its

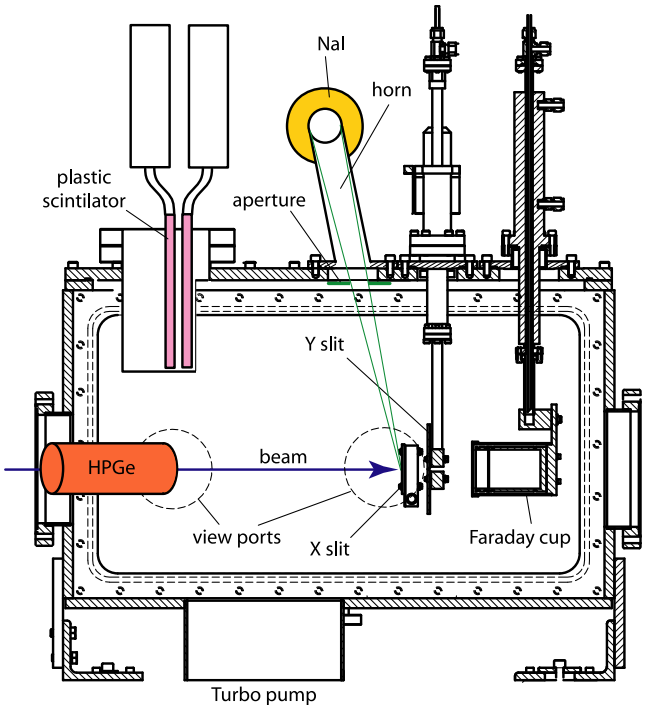

Fig. 3. Radiation detectors at the DRAGON mass slits chamber. Two plastic scintillators are mounted inside a recess with a thin stainless steal wall on the side facing the mass slits. The HPGe detector (located external to the chamber) was pointed at the mass slits through a view port, while the two NaI detectors were positioned about the'horn' and oriented at 180° to each other.

1836 keV γ-ray line. The detector efficiency was calibrated with reference sources. The $^{26\,m}$Al decay was monitored by detecting the positron decay. A 'horn' protruding above the mass slits box catches positrons from the ^{26m}Al decay under a well defined solid angle. Two 3 in. × 3 in. NaI detectors, oriented at 180° relative to each other and with the horn in the middle, detect the two 511 keV annihilation photos in coincidence. The absolute efficiency was determined from calibration measurement using a ^{22}Na source placed into the interior of the horn and the calculated solid angle coverage of the 'horn' (Fig. 3). The efficiencies of these detectors setups are in the 10^{-5}–10^{-6} range, enough to have a reasonable count rate from the present beam contamination (3×10^{-5} and 3×10^{-6} for ^{26m}Al and ^{26}Na, respectively). Note, in this experiment beam contamination was substantially reduced by the use of the resonant laser ion source TRILIS and fine-tuning of the high resolution mass separator ion optics following the ion source; for the latter the positron signal severed as a feedback for the tuning process.

6. DRAGON ionization chamber

Most of the measurements at DRAGON made use of a double-sided silicon strip detector (DSSSD) as the end detector. The reason for that is the position resolution over the size of 5 × 5 cm^2, the good energy resolution for light

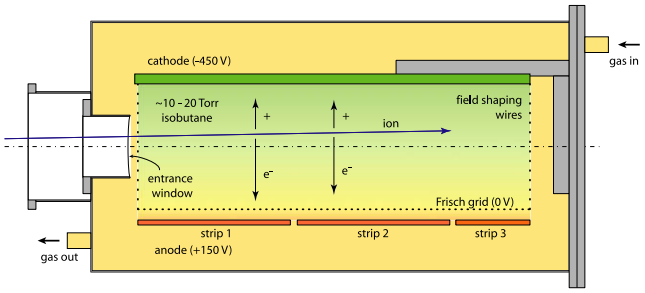

Fig. 4. Layout of the DRAGON ionization chamber.

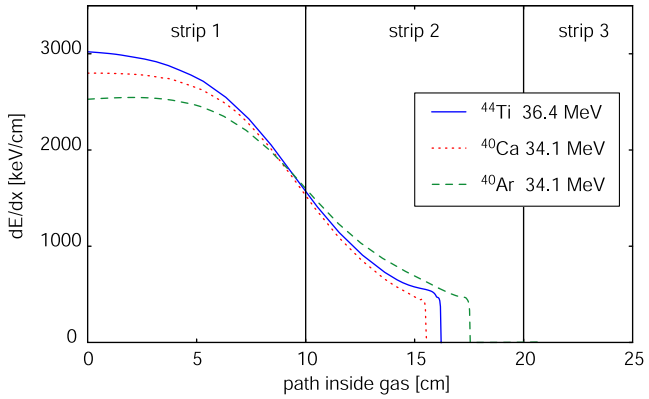

Fig. 5. Stopping power of ^{44}Ti, ^{40}Ca and ^{40}Ar ions as a function of the path inside the ionization chamber filled with 19 Torr isobutane. The energy of the ions is based on an initial beam energy of $E_{in} = 1000$ A keV: ^{44}Ti recoils have $40^2/44^2 E_{in}$; the energy of the ^{40}Ca and ^{40}Ar ions is for the next lower charge state (12^+) and same momentum as the recoils in charge state 13^+. The energy loss in the 130 μm Mylar window is taken into account. The calculation is based on stopping power tables from SRIM2006 [9].

ions and the ease of use. However, for heavier ions ($A \gtrsim 20$) at low energies ($E \lesssim 0.5$ A MeV) a gas ionization chamber has several advantages over the DSSSD. First, it provides better energy resolution as the dead layer can be reduced with the use of a thin entrance window, and second, a segmented anode allows energy-loss measurements and thus provides additional information for recoil identification and also isobar separation.

Fig. 4 shows the schematic setup of the DRAGON ionization chamber. It consists of gas volume of 25 cm length filled with isobutane and separated from the upstream beam line by a thin entrance window (130 μg/cm^2 Mylar or grid-supported 55 μg/cm^2 poly-propylene) of 50 mm diameter. Ions entering the ionization chamber lose energy in the gas according to their stopping power dE/dx, which depends on energy E, mass A and nuclear charge Z of the ions. The ionization products along the path of the ions are separated by a moderate electric field (50 V/cm). Equipotential electrodes and wires surrounding the active gas volume ensure a homogeneous electric field. Electrons are collected at the anode, which is segmented into two 10 cm sections and a 5 cm section at the end of the chamber. A Frisch grid electrically separates the anode from the collecting volume. The gas pressure is adjusted to stop the ions before the end of the second segment. The total energy is measured as the sum of all segments. In case of ^{40}Ca at 1.1 A MeV we achieved a resolution of 1.2% FWHM.

The resolving power of the ion chamber was essential for the measurement of the ^{40}Ca(α, γ)^{44}Ti reaction [8] because beam suppression is reduced due to the relatively high mass and mass to charge state ambiguities (see [3] for details). The layout of the anode strips was chosen for best identification of recoils and isobar separation. As the signal on the anode strips is proportional to the integrated stopping power, the anode is segmented at the position where the stopping power curves cross (Fig. 5). In that way isobaric beam contamination from ^{40}Ar could be clearly identified and monitored during the measurement time.

7. Outlook and summary

We are currently in the process of upgrading the detector end station with a local time-of-flight measurement based on two MCP detectors looking at secondary electrons from thin carbon foils. An electrostatic mirror deflects the electrons out of the beam axis onto the MCP detectors. With the anticipated flight path of 57 cm between the two foils the flight time for example mass 20 at 0.5 A MeV is about 60 ns and the expected difference between proton capture recoils and beam ions is about 3 ns. Thus, with a sub-ns time resolution they should be well separated even at lower energies where the resolution of energy detectors is not sufficient for a clear recoil identification.

Since its installation in 2001 the DRAGON facility has been used for several important reactions for nuclear astrophysics. Due to the different requirements for the experiments, several improvements to the original setup have been made. These additions will also be useful for upcoming experiments at DRAGON and might be relevant for other similar facilities, in particular at radioactive beam facilities.

Acknowledgement

The work was supported in part by a grant from the Natural Science and Engineering Research Council of Canada.

References

[1] D.A. Hutcheon et al., Nucl. Instr. and Meth. A. 498 (2003) 190.
[2] S. Engel et al., Nucl. Instr. and Meth. A. 553 (2005) 491.
[3] D. Hutcheon et al., Nucl. Instr. Meth. B 266 (2008) 4171.
[4] C. Matei et al., Phys. Rev. Lett. 97 (2006) 242503.
[5] C. Ruiz et al., Phys. Rev. Lett. 96 (2006) 235501.
[6] C. Vockenhuber et al., Nucl. Instr. and Meth. B 259 (2007) 688.
[7] J.M. D'Auria et al., Phys. Rev. C 69 (2004) 065803.
[8] C. Vockenhuber et al., Phys. Rev. C 76 (2007) 035801.
[9] J.F. Ziegler, The stopping and range of ions in solids, <http://srim.org> (2007).